Dynamics and Stability of E-Cadherin Dimers

Fabien Cailliez and Richard Lavery
Laboratoire de Biochimie Théorique, CNRS UPR 9080, Institut de Biologie Physico-Chimique, Paris 75005, France

ABSTRACT The extracellular domains of cadherins are known to play a major role in cell adhesion, although the structures involved in this process remain unclear. We have used molecular dynamics to characterize the conformational and thermodynamic properties of two of the dimer interfaces identified in E-cadherin crystals and involving the two outermost exodomains (EC1 and EC2): a dimer involving exchange of the N-terminal strand (referred to as the ''swapped'' dimer) and a ''staggered'' dimer involving an EC1-EC2 interface. The results show that the staggered dimer involves a much smaller interface area and is notably less stable than the swapped dimer. It is also found that, despite its stability, the swapped dimer undergoes a conformational transition leading to a structure closer to that experimentally observed for the homologous C-cadherin. Finally, comparing the simulated dimer structures with the sequences of E-, C-, and N-cadherins shows that the swapped dimer interface involves surprisingly few residues that vary from family to family and notably no changes between the E- and C-cadherin exodomains.

INTRODUCTION

Cadherins are one of the most important families of cell adhesion proteins. They can be found in many multi-cellular organisms, where they play important roles in embryogenesis and tissue maintenance (1,2). The most studied cadherins belong to the so-called type I classical subfamily, which includes the homologous C-, E-, N-, and P-cadherins. A critical component of these molecules is the five-domain extracellular (EC) portion (3). These five domains fold independently into seven-stranded β-sandwich topologies (the domains are numbered from the outermost N-terminal, EC1–EC5). Each interdomain junction is associated with three calcium ion binding sites; and a variety of experimental data—including electron microscopy on both complete E-cadherin EC domains and on EC1-2 fragments, the minimal unit necessary for intercellular adhesion (4)—has shown that calcium binding is necessary for the rigidity of these junctions and the overall ''rod-like'' conformation of the exodomain (5,6). Calcium binding also turns out to be necessary for cadherins to play their role in cellular adhesion (7–10). Molecular dynamics (MD) simulations on E- and C-cadherins have confirmed the vital role of calcium binding (11,12), although our studies on the EC1-2 domains of E-cadherin also point to the fact that the most exposed Ca^{2+} does not seem to be essential in stabilizing this junction.

Exactly how classical cadherins dimerize is still not clear. The involvement of at least two types of cadherin-cadherin contacts in adhesion has been deduced from electron microscopy experiments (10,13). These involve contacts between EC domains belonging to cadherins of the same cell (*cis* interactions) and contacts between cadherins of interacting cells (*trans* interactions). These studies do not yet have sufficiently high resolution to reveal the atomic details of the interactions; however, data obtained from mutagenesis experiments have emphasized the role of several amino acids. Among these, mutations of Trp-2 and Ala-80 are known to abolish *trans* interactions but do not affect *cis* interactions (10). Two recent studies have clarified the role of Trp-2 and also shown the importance of Glu-89 in adhesion (14,15).

Another source of information on cadherin interactions comes from crystallographic studies of the truncated exodomains and notably from the observed intermolecular contacts. The first high-resolution structures of cadherins concerned the EC1 domain of E-cadherin (16) and of N-cadherin (17). Both structures show virtually identical folded domains, but the second study also brought to light two different interfaces between EC1 domains: a parallel interface, proposed to be involved in *cis* interactions between molecules from a single cell, and an antiparallel contact, presumably representing an intercellular *trans* interaction. A remarkable feature of the parallel interface is a strand exchange allowing the Trp-2 residue from one monomer to be inserted into the hydrophobic pocket of the partner molecule (containing, among other residues, Ala-80), corresponding to a so-called swapped dimer. The importance of this type of interaction for adhesion is supported by the mutagenesis experiments cited above. These observations led to the so-called zipper model for cadherin interactions (17). Subsequent crystallographic structures of EC1-2 fragments of E-cadherin (Protein Data Bank code 1EDH and 1FF5) led to different conclusions (10,18).

In both of these studies, two EC1-2 monomers form an X-shaped dimer with parallel interactions between the EC1 modules and an interface that spreads into the calcium-binding junction region of the fragments. The parallel nature of this interaction once again suggests a model for *cis* interactions. In the 1FF5 structure, the Trp-2 residue of each molecule is in its own hydrophobic pocket, unlike the strand-exchanged conformation of the earlier ''zipper'' model. (The

Submitted April 14, 2006, and accepted for publication August 24, 2006.

Address reprint requests to Richard Lavery, Tel.: 33-1-58-41-50-16; Fax: 33-1-58-41-50-26; E-mail: rlavery@ibpc.fr.

0006-3495/06/12/3964/08 $2.00

doi: 10.1529/biophysj.106.087213

situation of Trp-2 is unclear in the 1EDH structure because the N-terminal residues are not resolved.) We term this structure a ''nonswapped'' dimer. It is important to note that both 1FF5 and 1EDH structures have been obtained from E-cadherin constructs having either one or two extra residues at the N-terminus. Other studies have shown that elongating the N-terminus of cadherin perturbs interactions and can lead to the loss of adhesive properties (8,15,19). The nonswapped dimer has therefore not been observed with the biologically active form of the N-terminal and must currently be considered hypothetical. It is noted in passing that an N-cadherin EC1-2 dimer, with a correctly processed N-terminal, has been obtained and this structure shows a disordered rather than a swapped strand (20). However, in light of the other evidence available, the authors of this study concluded that this interface was probably not biologically relevant.

Concerning intercellular *trans* interactions, a more recent E-cadherin EC1-2 structure (8) reveals two molecules interacting via their EC1 domains in what approaches an antiparallel arrangement. In this structure (Protein Data Bank code 1Q1P), strand exchange involving Trp-2 is again observed. This structure also resembles another recent result obtained with the complete exodomain of C-cadherin (3).

In addition to these interactions, another interface is observed between the EC1-2 fragments in many of the structures already cited. This interface involves a parallel contact between the EC1 module of one fragment and the EC2 module of its partner (hereafter termed a ''staggered'' interaction). Although this interaction has often been considered to be a simple crystal contact, some authors have suggested its possible involvement in *cis* interactions (3).

On the basis of these experimental results, a number of different, and sometimes contradictory, models of cadherin-driven adhesion have been put forward. Although there is still no definitive evidence in favor of any single model, the involvement of strand-exchanged dimers has received support from several directions, including recent electron tomography studies of desmosomal cadherins at mouse epidermal cell interfaces which show that *cis* and *trans* interactions could both be modeled using strand-exchanged dimer structures (21).

As concerns the vital role of cadherins in selective cell binding, the experimental data are again complex. Although there is a very high degree of sequence homology between the various classical cadherins, it was initially thought that homophilic interactions were strongly favored. More recent data show that heterophilic interactions can be formed and rather suggest that selectivity results from the collective effects of many individual dimer interactions (22,23). One model shows that very small differences in affinity for the swapped dimers could be amplified in this way (24). The implication of the swapped dimer for the selectivity of classical cadherin interactions has been demonstrated in a recent publication by Patel and co-workers (25). In this study, structures of type II cadherin ectodomains have been obtained using x-ray crystallography. The swapping mechanism for type II cadherins involves a second tryptophane (Trp-4), which is not present in the type I family (such as E-, N-, and C-cadherins). This study brings further evidence of the involvement of the EC1 domain in cadherin selectivity although, given the small sequence differences between the different cadherins, selectivity of either type I or type II cadherins remains difficult to explain on a purely structural basis. In this context, it should be remarked that biomembrane force probe experiments (26,27) have suggested that selectivity may in some cases be related to kinetic rather than thermodynamic factors.

In light of these questions and in the absence of definitive structural data, molecular simulations may be able to contribute to a better understanding of the various cadherin interactions discussed above. We have previously used this approach to study both EC1-2 monomers and the hypothetical nonswapped EC1-2 dimer (with a correctly processed N-terminal). We now present a comparative study of the dynamics and stability of the remaining interfaces discussed above, namely, the swapped and staggered dimers (Fig. 1). All calculations involve EC1-2 fragments of E-cadherin. The results show that the staggered dimer interface is clearly much less stable than the swapped or the (hypothetical) nonswapped forms. Interestingly, the swapped dimer shows a structural change which leads to a transition from the form observed crystallographically for E-cadherin (8) toward that

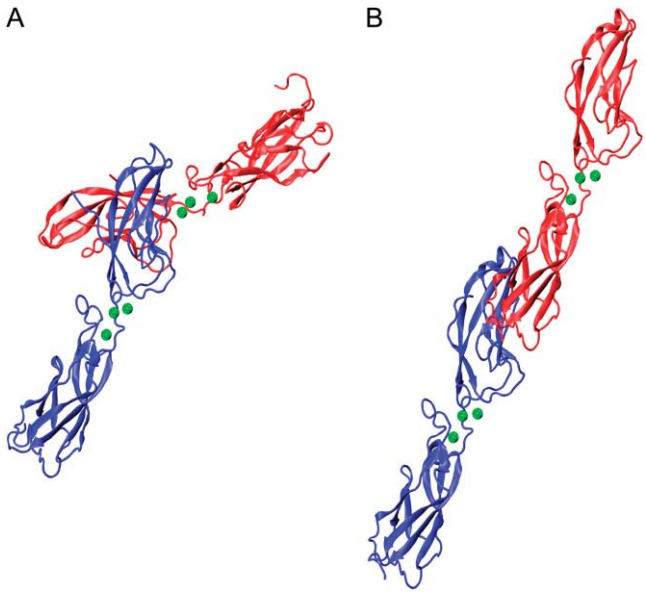

FIGURE 1 Crystallographic structures of the EC1-2 dimers of E-cadherin. The two-domain monomers are shown in red and blue, and junction-bound calcium ions are green. (*A*) Swapped dimer (1Q1P) involving an antiparallel interaction between two EC1 domains. (*B*) Staggered dimer (1FF5, but also present in 1Q1P) involving a parallel interaction between an EC1 domain (of the *blue* monomer) and an EC2 domain (of the *red* monomer). Figs. 1, 4, and 5 were produced using visual molecular dynamics (43).

seen for C-cadherin (3). We have also made an analysis of the residues involved in the cadherin interfaces which allows us to speculate on their possible role in cell sorting on the basis of the sequence differences between the E-, C-, and N-cadherins.

MATERIALS AND METHODS

Cadherin dimer construction

Two different EC1-2 dimers have been examined in this study. The swapped dimer was built from the crystallographic structure 1Q1P by applying a crystallographic symmetry operation on chain A. This structure lacks the residue Asp-1 and also the residues 214–218. These residues have been added using the module *Tleap* from the AMBER software (28) (the conformation of the four C-terminal residues was copied from the 1FF5 crystal structure). For the staggered dimer, the structure was obtained by applying the appropriate crystallographic symmetry operations to chain A of the 1FF5 crystal structure. It could have also been obtained from the 1Q1P monomer (yielding a conformation within a Cα root mean-square deviation (RMSD) of 1.9 Å from the 1FF5 result), but this structure naturally has a solvent-exposed N-terminal and would again require building in missing residues.

Setting up the simulations

The pKa of all the ionizable residues were computed using WHATIF (29). All of them were found to be in their standard ionization state at neutral pH, leading to a total charge of -20 for each dimer (taking into account the six bound Ca^{2+} ions). Each dimer conformation was solvated with TIP3P water molecules (30) and 20 K^+ ions were added to neutralize the simulation cells. K^+ and Cl^- ions were further added to achieve an ionic concentration of $\sim$0.15 mol L^{-1}. The monovalent ions were randomly placed around the solute using the *Ptraj* module of the AMBER package. An octahedral water box was used for the swapped dimer, but a rectangular box was chosen for the staggered dimer due to the elongated nature of this conformation (Fig. 1). In all cases, a minimum distance of 10 Å was imposed between the solute and the edge of the box. This led to systems comprising $\sim$230,000 and 147,000 atoms, respectively, for the swapped and staggered dimers.

MD simulations

MD simulations were carried out using the *Pmemd* module of the AMBER 8 package (28) with the parm99 force field (31). Calculations employed the periodic boundary conditions described above, and the particle mesh Ewald method (32,33) was used to treat long-range electrostatic interactions with a real-space cutoff of 9 Å. SHAKE restraints (34) were applied to all bonds containing hydrogen atoms, and integrations were performed with a 2 fs time step. Both dimers were first submitted to several thousand steps of minimization using 25 kcal $mol^{-1}/Å^{-2}$ quadratic restraints on all atoms of the solute. The temperature was then increased to 300 K within 10 ps and stabilized during 40 ps, with the solute still restrained. The restraints were then progressively decreased from 5 to 0.5 kcal/mol^{-1} $Å^{-2}$, with 2000 steps of minimization and 25–50 ps MD simulation at each stage. Lastly, 50–100 ps of unrestrained dynamics were performed before the production phase. In the case of the staggered dimer, quadratic restraints were applied to two atoms of one monomer constituting a bond lying nearly parallel to the longest axis of the rectangular box (Cα-C′ Ile-242) to prevent the overall rotation of the solute. Production runs were carried out for 12.5 ns for both dimers. Comparisons were made with the 10 ns simulation of the E-cadherin monomer discussed in our earlier work (11).

Conformational analysis

Standard conformational analysis was carried out using the *Carnal* and *Ptraj* modules of the AMBER package as well as the Profit software developed by A. C. R. Martin (http://www.bioinf.org.uk/software/profit). Accessible surface areas (ASAs) were computed using a Korobov grid of 610 points on the surface of each atom and a probe sphere of 1.4 Å radius (11,35). The interface area of a dimer is defined as the difference between the sum of the ASA of the isolated monomers minus the ASA of the dimer. The bending angle and torsion angles between the two EC domains were probed during the simulations using the geometrical definition described in our preceding publication (11). Briefly, this involves defining an optimal axis for β-barrel of each EC domain. The bending angle is the angle formed by these axes, whereas the torsion angle is calculated between vectors perpendicular to the domain axis pointing toward two β-strand residues chosen to give an angle close to zero in the EC1-2 starting structure.

Free energy estimates

Free energy estimates have been computed using the so-called molecular mechanics Poisson-Boltzmann surface area (MM-PBSA) approach (36,37). This involved extracting 500 regularly spaced snapshots from the last 5 ns of the monomer and the two dimer simulations. It should be noted that in the monomer simulation, the Trp-2 is included in the hydrophobic pocket of its own EC1 domain. Thus, when calculating free energy of dimerization for the swapped dimer, the effect of strand swapping is taken into account. Gas-phase enthalpies were then calculated using parm99 parameters. The polar part of the solvation free energies was computed using a numerical Poisson-Boltzmann solution with a grid spacing of 0.67 Å, a solute dielectric of 1, a solvent dielectric of 78.5, and a salt concentration of 0.15 mol L^{-1}. A surface area term with a surface tension of 0.005 kcal/mol^{-1} $Å^{-2}$ was calculated to account for the nonpolar contribution to solvation free energy. Estimates of solute translational and rotational entropy were derived from classical statistical thermodynamics (38), whereas conformational entropies were calculated using normal mode calculations (36) for 10 snapshots sampled uniformly from the last 5 ns of each simulation. Conjugate gradient minimizations, carried out before normal mode calculations, were converged to 0.0001 kcal/mol^{-1} $Å^{-1}$ using a 4 r distance-dependent dielectric function.

RESULTS AND DISCUSSION

Structural analysis of the EC1-2 dimers

As in our earlier studies (11), the EC1-2 monomer conformations (in the presence of three bound calcium ions) are found to be very stable throughout the MD simulations, with RMSD deviations with respect to the starting structures staying below 2 Å (or 3 Å in the simulation of the swapped dimer, due to movements of the N-terminal residues). The results in Table 1 also show that this stability is reflected in the average values and the fluctuations of the bending and torsion angles connecting the EC1 and EC2 domains, which remain close to the values found in the earlier monomer simulation. It is however remarked that the bending angles are lower than those found in the crystal structures, presumably because of the absence of crystal packing constraints. These results show that the EC1-2 monomer junctions are quite rigid and largely unaffected by the existence, or the type, of the dimer interface.

The same rigidity does not apply to the overall fluctuations within the dimers. Fig. 2 presents the evolution of the RMSD

TABLE 1 Average values and standard deviations of the bending and torsion angles between the EC1 and EC2 domains during the MD simulations

Simulation	Time interval (ns)	Bending angle (°)	Torsion angle (°)
Monomer	2.5–10	137 ± 6 (154)	−18 ± 9 (−16)
Swapped dimer	2.5–12.5	141 ± 7 (148)	−18 ± 8 (−21)
		134 ± 9 (148)	−19 ± 8 (−21)
Staggered dimer	2.5–12.5	138 ± 8 (154)	−29 ± 9 (−16)
		152 ± 9 (154)	−17 ± 9 (−16)

Data from the RMSD time series were used to determine the intervals in which the structures were stable enough to allow averaging. The values in brackets correspond to the crystal structures.

of the dimers with respect to the corresponding crystallographic structures during the two simulations. Although the staggered dimer has a very extended conformation (Fig. 1), it deviates relatively little from the starting structure, with RMSD values oscillating around 4 Å. In contrast, the swapped dimer rapidly moves away from the starting conformation, leading to RMSD values up to 12 Å.

Another way of analyzing these dimers is to calculate their interface areas. The results show two clear features. The first concerns the range of the average interface areas. The swapped and staggered dimers both exhibit relatively small areas of ~1700 Å^2 and 1200 Å^2, respectively. These values are both below the typical areas for protein-protein interfaces of ~2400 Å^2 (39,40), which, in passing, was also the value found for the hypothetical nonswapped dimer in our earlier studies (11). Second, as shown in Fig. 3, both dimers show significant changes in interface as the simulations progress. This evolution results in an increase of ~200 Å^2 for the swapped dimer during the last 5 ns but to a decrease of ~200 Å^2 for the staggered dimer during the same period.

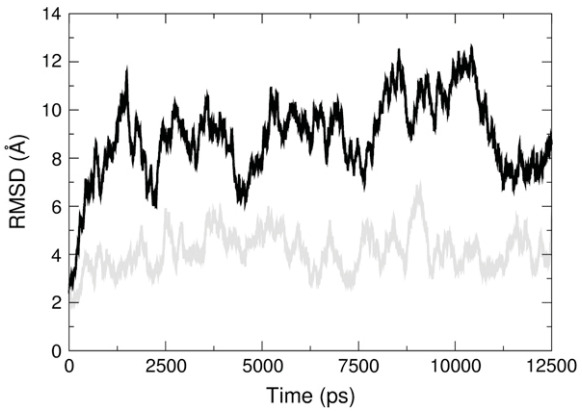

FIGURE 2 Evolution of the dimer structures during the simulations. RMSD (for all heavy atoms) with respect to the crystallographic starting structures during the MD simulations of the swapped dimer (*thick black line*) and the staggered dimer (*shaded line*).

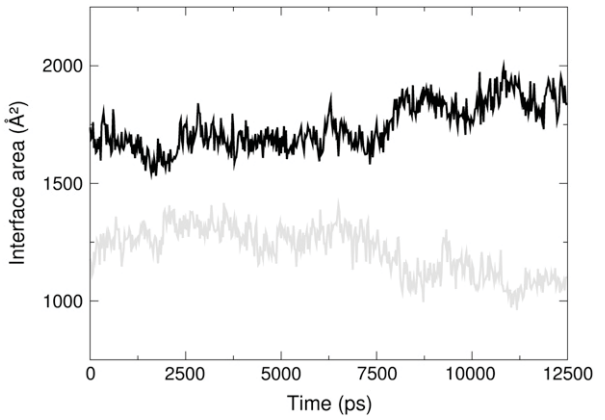

FIGURE 3 Evolution of the dimer interfaces during the simulations. Dimer interface area between the EC1-2 monomers during the simulations of the swapped dimer (*thick black line*) and the staggered dimer (*shaded line*).

Conformational change in the swapped dimer

What is the nature of the important changes in the swapped dimer? Given the results already presented, it clearly involves the dimer interface rather than the monomer conformation and, as already noted, the interface area actually increases during the simulation. The overall evolution is shown in Fig. 4, which compares the crystallographic starting conformation with the mean structure derived from the last 2.5 ns of the simulation. The dimer interface has been significantly modified, moving toward the extremities of the interacting EC1 domains, although the relative orientation of the monomer axes has not been strongly affected. A more detailed view is shown in Fig. 5, where it can be seen that the process begins with the formation of new contacts between the N-terminal strands of the EC1 domains (involved in the strand exchange) and their more complete insertion into the β-barrel of their own domains. This is followed by the

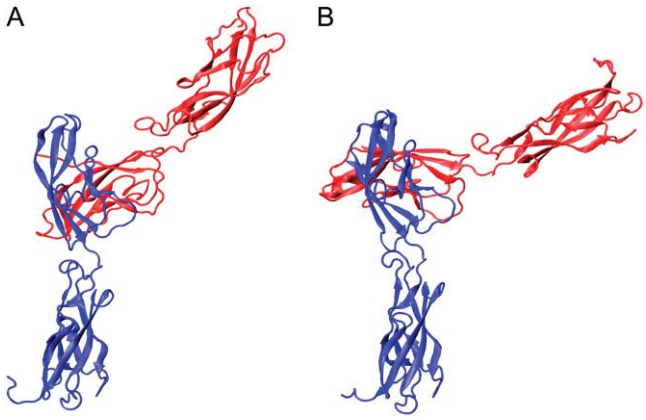

FIGURE 4 Conformational change in the swapped dimer. Changes in the swapped dimer during the MD simulation: (*A*) Crystallographic starting conformation (1Q1P); (*B*) average structure over the last 2.5 ns of the simulation.

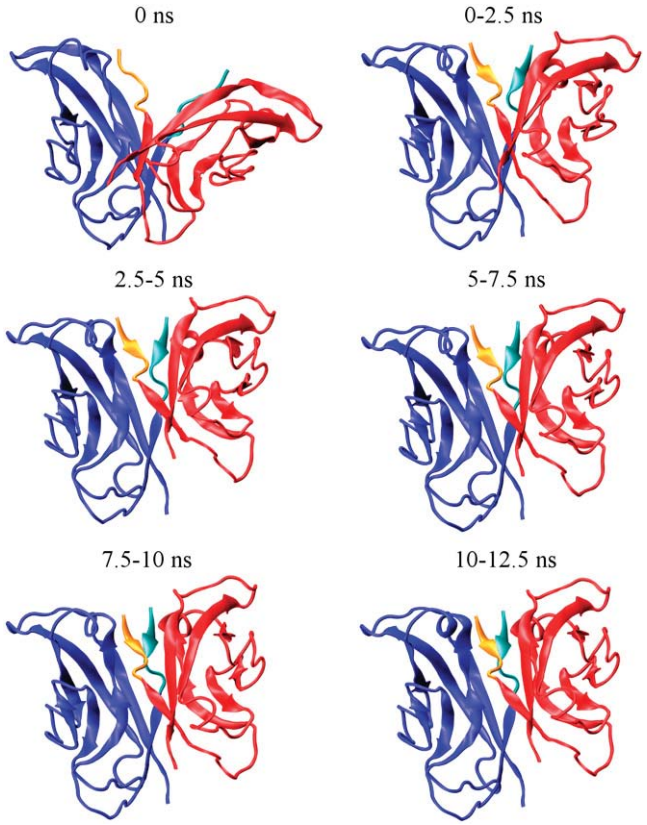

FIGURE 5 Evolution of the EC1-EC1 interactions over the course of the swapped dimer simulation. The interacting EC1 monomers are shown in red and blue. The first six residues of each monomer involved in strand exchange are shown in cyan for the blue monomer and orange for the red monomer. Each picture, except the starting structure at 0 ns, is averaged over a 2.5-ns segment of the MD trajectory. Secondary structures are calculated using the Stride option of visual molecular dynamics (43).

mutual approach of the two N-terminal strands to create a short, parallel β-ribbon.

Interestingly, the first phase of this evolution, with each N-terminal integrated into its own β-barrel, resembles the crystallographic interface of the swapped dimer of C-cadherin (3). Although E- and C-cadherin are highly homologous (65% for the EC1-2 fragment and 70% for the EC1 domain), the latter exhibits a somewhat larger swapped interface, corresponding to the evolution we see in the E-cadherin dimer. The RMSD time series of our simulation, shown in Fig. 6, demonstrates that the E-cadherin dimer rapidly moves away from its starting conformation and approaches that of C-cadherin. This interface rearrangement takes the structure 5 Å away from its starting point in terms of RMSD, whereas, after the first 500 ps of simulation, it remains within 2.5 Å of the C-cadherin structure.

Fig. 7 shows another way to analyze this evolution using two interatomic distances. The first, between residues Val-3 and Met-92 of a single EC1 domain (d_{3-92}), reflects the insertion of the N-terminal strand into the β-barrel of its own domain, whereas the second, between the Trp-2 residues of each monomer ($d_{2-2'}$), reflects the formation of the interchain β-sheet. The figure shows that both these values almost immediately adopt smaller values than those in the E-cadherin crystallographic conformation. As the simulation progresses, d_{3-92} and $d_{2-2'}$ both stay close to the values seen in C-cadherin; however, $d_{2-2'}$ finally moves to still smaller values (after 8 ns), reflecting the fact that the formation of an N-terminal β-ribbon is absent in the C-cadherin structure. It should be remarked that the tendency to move away from the structure found for E-cadherin is not related to the use of the biologically active form of the N-terminal in our simulations (that is, without any residues preceding Asp-1), since this is also the form studied crystallographically.

Free energy calculations

Although we have seen that both the swapped and staggered dimers show structural changes during the MD simulations, it is not easy to deduce the thermodynamic consequences of these changes. We have therefore estimated the stability of the two dimer interfaces using the MM-PBSA approach described in the Methods section and based on the analysis

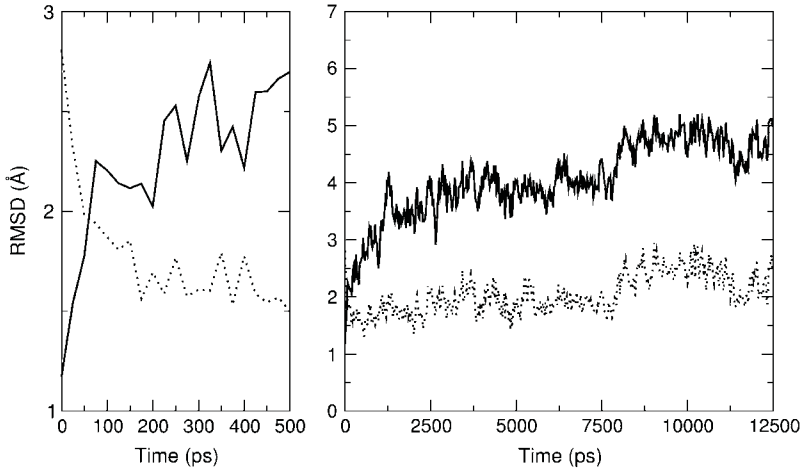

FIGURE 6 Backbone RMSD for the interacting EC1 domains during the swapped dimer simulation. The solid line shows values calculated with respect to the E-cadherin starting structure and the dotted line, the values with respect to a C-cadherin swapped dimer. The left-hand plot shows a close-up view of the first 500 ps of the MD simulation.

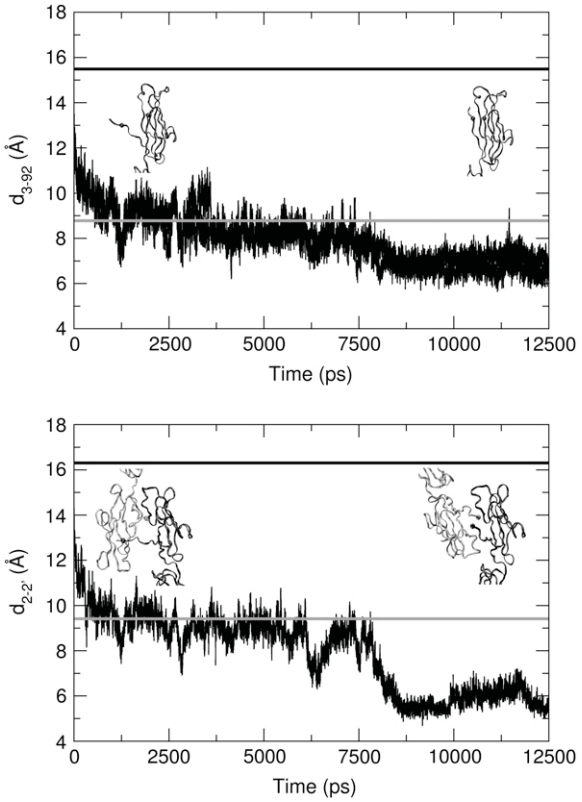

FIGURE 7 Formation of new β-strand contacts at the strand-exchanged dimer interface. Changes in the EC1 swapped dimer interface reflected by the distance between the Val-3 and Met-92 residues (*upper plot*) and between the Trp-2 residues of the two domains (*lower plot*). The horizontal solid and shaded lines show the corresponding distances in the crystallographic E- and C-cadherin swapped dimer structures.

of an ensemble of snapshots taken from the MD simulations. The dimerization free energies, with respect to EC1-2 monomers (with Trp-2 in its own hydrophobic pocket), are presented in Table 2. Although the total binding free energies are clearly overestimated, the relative values are informative. Two main features stand out. First, the staggered dimer, in line with its small interface and conformational fluctuations, is by far the least stable conformation, having a binding free energy much below the other form. Although its role in cadherin-driven adhesion cannot be completely ruled out, this interface is clearly the weakest. Second, despite the significant change in conformation, the swapped dimer remains a very stable structure and is clearly a good candidate for the formation of strong E-cadherin interactions. These values can be compared with that value of -29 kcal mol^{-1} obtained previously for the hypothetical nonswapped dimer (11). The fact that this value is well below that for the swapped dimer may explain the preference for the latter in the presence of a correctly processed N-terminal.

TABLE 2 Free energies ΔG (in kcal mol^{-1}) for dimer formation and their component contributions calculated with the MM-PBSA method

Contribution	Swapped dimer	Staggered dimer
ΔH_{int}	−9	−15
ΔH_{vdW}	−28	−50
ΔH_{coul}	289	397
ΔG_{solv}	−325	−374
ΔG_{elec}	−36	23
ΔG_{surf}	−1	−3
$-T\Delta S$	34	34
ΔG	−41	−11

Dimer interfaces and cadherin specificity

Lastly, we consider whether the simulations of the different E-cadherin dimer interfaces can help in understanding the specificity of dimer interactions. To analyze the potential role of sequence differences between E-, C-, and N-cadherins, we have first identified those residues of E-cadherin which contribute significantly to each type of dimer interface. Interface residues were defined as those with >50% of buried surface area with respect to the isolated monomers and a total buried area of at least 10 Å^2 per residue. The number of residues making up each type of interface is seen to be unrelated to stability since the staggered and the swapped dimers are similar in this respect. As expected, despite the thermal fluctuations inherent to the MD simulations, the monomer contributions to the swapped dimer interface are seen to be virtually symmetric. This is naturally not the case for the staggered interface where the monomers participate via the EC1 and EC2 domains, respectively.

If we now assume that C- and N-cadherins can adopt identical dimer conformations, we can ask whether the resulting changes within their aligned sequences appear to be important for each type of dimer. The results are shown in Table 3 by the italics, which indicate residues contributing significantly to the dimer interfaces but differing in sequence for at least two of the three cadherins compared. On this basis, the weak staggered interactions appear to be significantly sequence dependent. In contrast, the strong swapped dimer appears to have a very limited dependence on sequence, and notably, although there are three residues differing between E- and N-cadherin (of which Lys-25 makes a particularly important contribution to the interface), no differences are found between E- and C-cadherin. This observation is in line with several experiments showing specific cell aggregation in the case of E- and N-forms (22) but no discrimination in the case of the E- and C-forms of cadherin (41). It also correlates with our finding that, during MD simulations, the swapped dimer of E-cadherin evolves to resemble that of C-cadherin. It should however be repeated that this analysis concerns buried surface areas and not energy contributions and also does not take into account potential structural changes induced by residues outside the dimer interface. It, however, supports the idea that selectivity between different cadherins relies on small and subtle thermo-

TABLE 3 Buried surface area, BSA (Å^2), of residues belonging to the monomers forming the swapped and staggered dimers of E-cadherin, based on averages over the last 5 ns of the corresponding MD simulations

	Swapped					Staggered				
	Residue	BSA	E	C	N	Residue	BSA	E	C	N
I	2	261	W	W	W	***175***	***79***	***L***	***I***	***V***
	25	***90***	***K***	***K***	***R***	***177***	***63***	***S***	***T***	***A***
	5	90	P	P	P	123	61	P	P	P
	3	72	V	V	V	124	54	G	G	G
	26	33	S	S	S	166	41	N	N	N
	92	***31***	***M***	***M***	***I***	***176***	***36***	***T***	***G***	***A***
	164	35	T	T	T	***173***	***17***	***S***	***S***	***I***
II	2	251	W	W	W	84	91	N	N	N
	1	112	D	D	D	***55***	***73***	***R***	***W***	***P***
	25	***99***	***K***	***K***	***R***	85	59	G	G	G
	5	86	P	P	P	79	58	H	H	H
	3	71	V	V	V	81	53	V	V	V
	89	50	E	E	E	***83***	***48***	***S***	***E***	***I***
	23	***46***	***Q***	***Q***	***R***	37	46	S	S	S
	92	***35***	***M***	***M***	***I***	***35***	***44***	***F***	***Y***	***R***

Only those residues buried by >50% and contributing >10 Å^2 to the interface area are included, and residues are listed in decreasing order of their BSA. The equivalent residues in C- and N-cadherins are listed after a multiple sequence alignment using ClustalW with standard input parameters. Italics indicate residues that differ between at least two of the classical cadherin families.

dynamic contributions (24) and could conceivably involve kinetic factors (26,27).

CONCLUSIONS

We have used MD simulations to investigate conformational and thermodynamic properties of two EC1-2 dimers of E-cadherin derived from crystallographic structures. In both cases, we have observed that the monomers show little deformation and, in the presence of bound calcium ions at the domain junctions, retain their initial ''rod-like'' conformations no matter which dimer interface is formed. However, the different interfaces do not exhibit the same rigidity. The swapped dimer undergoes important structural modifications that lead to a reinforcement of the interface and to a conformation closer to that experimentally observed for C-cadherin. One can speculate that this could be due to crystallographic packing effects acting on the E-cadherin starting structure. In the case of the staggered dimer, the initially small interface area is further decreased during the simulation. Binding free energy estimates show that the swapped dimer is much more stable than the staggered form. This supports the idea that the staggered interface is probably a simple crystal contact rather than a functional interface. However, it is necessary to remain cautious since cadherin-cadherin interactions are notoriously weak (5,42) and adhesion relies on concentrated, multiple contacts (9). Lastly, an analysis of the residues participating in the dimer interfaces suggests that specificity must rely on subtle thermodynamic (or kinetic) factors in the case of the swapped dimer, which, although strongly formed, appears to have a virtually identical interface for both E- and C-cadherins and to show only limited variations for N-cadherin.

The authors thank Helene Feracci and Olivier Courjean (Curie Institute, Paris) for many helpful discussions on cadherin function and also the CINES center for the allocation of the supercomputer time used in carrying out these simulations.

REFERENCES

1. Takeichi, M. 1990. Cadherins: a molecular family important in selective cell-cell adhesion. *Annu. Rev. Biochem.* 59:237–252.
2. Yap, A. S., W. M. Brieher, and B. M. Gumbiner. 1997. Molecular and functional analysis of cadherin-based adherens junctions. *Annu. Rev. Cell Dev. Biol.* 13:119–146.
3. Boggon, T. J., J. Murray, S. Chappuis-Flament, E. Wong, B. M. Gumbiner, and L. Shapiro. 2002. C-cadherin ectodomain structure and implications for cell adhesion mechanisms. *Science.* 296:1308–1313.
4. Shan, W., Y. Yagita, Z. Wang, A. Koch, A. F. Svenningsen, E. Gruzglin, L. Pedraza, and D. R. Colman. 2004. The minimal essential unit for cadherin-mediated intercellular adhesion comprises extracellular domains 1 and 2. *J. Biol. Chem.* 279:55914–55923.
5. Alattia, J. R., J. B. Ames, T. Porumb, K. I. Tong, Y. M. Heng, P. Ottensmeyer, C. M. Kay, and M. Ikura. 1997. Lateral self-assembly of E-cadherin directed by cooperative calcium binding. *FEBS Lett.* 417:405–408.
6. Pokutta, S., K. Herrenknecht, R. Kemler, and J. Engel. 1994. Conformational changes of the recombinant extracellular domain of E-cadherin upon calcium binding. *Eur. J. Biochem.* 223:1019–1026.
7. Haussinger, D., T. Ahrens, H. J. Sass, O. Pertz, J. Engel, and S. Grzesiek. 2002. Calcium-dependent homoassociation of E-cadherin by NMR spectroscopy: changes in mobility, conformation and mapping of contact regions. *J. Mol. Biol.* 324:823–839.
8. Haussinger, D., T. Ahrens, T. Aberle, J. Engel, J. Stetefeld, and S. Grzesiek. 2004. Proteolytic E-cadherin activation followed by solution NMR and x-ray crystallography. *EMBO J.* 23:1699–1708.
9. Koch, A. W., K. L. Manzur, and W. Shan. 2004. Structure-based models of cadherin-mediated cell adhesion: the evolution continues. *Cell. Mol. Life Sci.* 61:1884–1895.
10. Pertz, O., D. Bozic, A. W. Koch, C. Fauser, A. Brancaccio, and J. Engel. 1999. A new crystal structure, Ca2+ dependence and mutational analysis reveal molecular details of E-cadherin homoassociation. *EMBO J.* 18:1738–1747.
11. Cailliez, F., and R. Lavery. 2005. Cadherin mechanics and complexation: the importance of calcium binding. *Biophys. J.* 89:3895–3903.
12. Sotomayor, M., D. P. Corey, and K. Schulten. 2005. In search of the hair-cell gating spring elastic properties of ankyrin and cadherin repeats. *Structure.* 13:669–682.
13. Tomschy, A., C. Fauser, R. Landwehr, and J. Engel. 1996. Homophilic adhesion of E-cadherin occurs by a co-operative two-step interaction of N-terminal domains. *EMBO J.* 15:3507–3514.
14. Harrison, O. J., E. M. Corps, T. Berge, and P. J. Kilshaw. 2005. The mechanism of cell adhesion by classical cadherins: the role of domain 1. *J. Cell Sci.* 118:711–721.
15. Harrison, O. J., E. M. Corps, and P. J. Kilshaw. 2005. Cadherin adhesion depends on a salt bridge at the N-terminus. *J. Cell Sci.* 118:4123–4130.
16. Overduin, M., T. S. Harvey, S. Bagby, K. I. Tong, P. Yau, M. Takeichi, and M. Ikura. 1995. Solution structure of the epithelial cadherin domain responsible for selective cell adhesion. *Science.* 267:386–389.

17. Shapiro, L., A. M. Fannon, P. D. Kwong, A. Thompson, M. S. Lehmann, G. Grubel, J. F. Legrand, J. Als-Nielsen, D. R. Colman, and W. A. Hendrickson. 1995. Structural basis of cell-cell adhesion by cadherins. *Nature*. 374:327–337.

18. Nagar, B., M. Overduin, M. Ikura, and J. M. Rini. 1996. Structural basis of calcium-induced E-cadherin rigidification and dimerization. *Nature*. 380:360–364.

19. Ozawa, M., and R. Kemler. 1990. Correct proteolytic cleavage is required for the cell adhesive function of uvomorulin. *J. Cell Biol.* 111:1645–1650.

20. Tamura, K., W. S. Shan, W. A. Hendrickson, D. R. Colman, and L. Shapiro. 1998. Structure-function analysis of cell adhesion by neural (N-) cadherin. *Neuron*. 20:1153–1163.

21. He, W., P. Cowin, and D. L. Stokes. 2003. Untangling desmosomal knots with electron tomography. *Science*. 302:109–113.

22. Patel, S. D., C. P. Chen, F. Bahna, B. Honig, and L. Shapiro. 2003. Cadherin-mediated cell-cell adhesion: sticking together as a family. *Curr. Opin. Struct. Biol.* 13:690–698.

23. Foty, R. A., and M. S. Steinberg. 2005. The differential adhesion hypothesis: a direct evaluation. *Dev. Biol.* 278:255–263.

24. Chen, C. P., S. Posy, A. Ben-Shaul, L. Shapiro, and B. H. Honig. 2005. Specificity of cell-cell adhesion by classical cadherins: critical role for low-affinity dimerization through beta-strand swapping. *Proc. Natl. Acad. Sci. USA.* 102:8531–8536.

25. Patel, S. D., C. Ciatto, C. P. Chen, F. Bahna, M. Rajebhosale, N. Arkus, I. Schieren, T. M. Jessell, B. Honig, S. R. Price, and L. Shapiro. 2006. Type II cadherin ectodomain structures: implications for classical cadherin specificity. *Cell.* 124:1255–1268.

26. Perret, E., A. Leung, H. Feracci, and E. Evans. 2004. Trans-bonded pairs of E-cadherin exhibit a remarkable hierarchy of mechanical strengths. *Proc. Natl. Acad. Sci. USA.* 101:16472–16477.

27. Bayas, M. V., A. Leung, E. Evans, and D. Leckband. 2006. Lifetime measurements reveal kinetic differences between homophilic cadherin bonds. *Biophys. J.* 90:1385–1395.

28. Case, D. A., T. A. Darden, T. E. Cheatham III, C. L. Simmerling, J. Wang, R. E. Duke, R. Luo, K. M. Merz, B. Wang, D. A. Pearlman, M. Crowley, S. Brozell, V. Tsui, H. Gohlke, J. Mongan, V. Hornak, G. Cui, P. Beroza, C. Schafmeister, J. W. Caldwell, W. S. Ross, and P. A. Kollman. 2004. AMBER8. University of California, San Francisco.

29. Vriend, G. 1990. WHAT IF: a molecular modeling and drug design program. *J. Mol. Graph.* 8:52–56.

30. Jorgensen, W. L. 1981. Transferable interatomic potential functions for water, alcohols and ethers. *J. Am. Chem. Soc.* 103:335–340.

31. Wang, J., P. Cieplak, and P. A. Kollman. 2000. How well does a restrained electrostatic potential (RESP) model perform in calculating conformational energies of organic and biological molecules? *J. Comput. Chem.* 21:1049–1074.

32. York, D. M., T. A. Darden, and L. G. Pedersen. 1993. The effect of long-range electrostatic interactions in simulations of macromolecular crystals—a comparison of the Ewald and truncated list methods. *J. Chem. Phys.* 99:8345–8348.

33. Cheatham, T. E., J. L. Miller, T. Fox, T. A. Darden, and P. A. Kollman. 1995. Molecular dynamics simulations on solvated biomolecular systems: the particle mesh Ewald method leads to stable trajectories of DNA, RNA, and proteins. *J. Am. Chem. Soc.* 117:4193–4194.

34. Ryckaert, J. P., G. Ciccotti, and H. J. C. Berendsen. 1977. Numerical integration of the Cartesian equations of motion of a system with constraints: molecular dynamics of *n*-alkanes. *J. Comp. Phys.* 23:327–341.

35. Lavery, R., A. Pullman, and B. Pullman. 1981. Steric accessibility of reactive centers in B-DNA. *Int. J. Quantum Chem.* 20:49–62.

36. Gohlke, H., and D. A. Case. 2004. Converging free energy estimates: MM-PB(GB)SA studies on the protein-protein complex Ras-Raf. *J. Comput. Chem.* 25:238–250.

37. Kollman, P. A., I. Massova, C. Reyes, B. Kuhn, S. Huo, L. Chong, M. Lee, T. Lee, Y. Duan, W. Wang, O. Donini, P. Cieplak, J. Srinivasan, D. A. Case, and T. E. Cheatham 3rd. 2000. Calculating structures and free energies of complex molecules: combining molecular mechanics and continuum models. *Acc. Chem. Res.* 33:889–897.

38. McQuarrie, D. A. 1976. Statistical Mechanics. Harper & Row, New York.

39. Chakrabarti, P., and J. Janin. 2002. Dissecting protein-protein recognition sites. *Proteins*. 47:334–343.

40. Bahadur, R. P., P. Chakrabarti, F. Rodier, and J. Janin. 2004. A dissection of specific and non-specific protein-protein interfaces. *J. Mol. Biol.* 336:943–955.

41. Niessen, C. M., and B. M. Gumbiner. 2002. Cadherin-mediated cell sorting not determined by binding or adhesion specificity. *J. Cell Biol.* 156:389–399.

42. Koch, A. W., S. Pokutta, A. Lustig, and J. Engel. 1997. Calcium binding and homoassociation of E-cadherin domains. *Biochemistry.* 36:7697–7705.

43. Humphrey, W., A. Dalke, and K. Schulten. 1996. VMD: visual molecular dynamics. *J. Mol. Graph.* 14:33–38.